Wavelets in all-electron density-functional calculations

Seungwu Han

Department of Physics and Center for Theoretical Physics, Seoul National University, Seoul 151-742, Korea
and Mechanics and Computation Division, Department of Mechanical Engineering, Stanford University, Stanford, California 94305

Kyeongjae Cho

Mechanics and Computation Division, Department of Mechanical Engineering, Stanford University, Stanford, California 94305

Jisoon Ihm

Department of Physics and Center for Theoretical Physics, Seoul National University, Seoul 151-742, Korea

We have developed an all-electron density-functional (AE-DF) program using the Mexican hat wavelet. The AE-DF program is applied to the *ab initio* all-electron calculations of small molecules as prototype systems, and the construction scheme of multiresolution support spheres is used to optimize the computational efficiency. Convergences are systematically demonstrated as a function of the number of resolution levels and support sphere sizes. Detailed analyses of H_2, CO, and H_2O molecules and the $1s$ core-ionized C*O and CO* molecules show good agreement with experiments and other theoretical works. The results indicate that one can gain computational efficiency by several orders of magnitude over the plane-wave-based methods in these molecules. [S0163-1829(99)00827-9]

Choosing an efficient and accurate basis set is a very important issue in modern *ab initio* electronic structure calculations. As the application areas are spreading over the conventional domains of bulk solid-state physics and quantum chemistry of small molecules to the surface chemical engineering, molecular biology, electronic devices, and nanotechnology, the *ab initio* method is emerging as a powerful tool for simulating real material systems. Conventional domains of solid state physics and quantum chemistry have developed two different types of the basis sets, plane waves (PW) and linear combination of atomic orbitals (LCAO), respectively. The PW basis set is suitable for the periodic systems and has the advantage of a systematic approximation of the complete basis expansion, whereas the LCAO basis set is suitable for the isolated molecules and requires only a small number of basis functions. In spite of the successful applications of these basis sets in the conventional domains, they are not well suited for efficient uses in newly emerging fields of applications.[1]

Reflecting this recent trend, a multitude of new approaches have been introduced to overcome the limitations of the PW and LCAO basis sets, and these include the adaptive Riemannian metric,[2] real-space grid methods,[3] and other $O(N)$ methods.[4] Recently, one of the authors introduced the wavelets as a spatially localized complete basis set for electronic structure calculations and demonstrated the potential efficiency of wavelets using hydrogenlike atoms and an H_2^+ molecular ion.[1] The spatially localized nature of the wavelet basis functions opens a new possibility for the development of a multiscale simulation tool in which the *ab initio*, atomistic, and continuum simulations can be seamlessly integrated.[5] The most recently developed multiscale simulation program [macroscopic-atomistic-*ab initio*-dynamics (MAAD)][5] uses the tight-binding (TB) method for the quantum description of Si since the PW basis cannot be used for

this application.[6] It is challenging to use the wavelet *ab initio* method in place of the TB so that the MAAD program can achieve the full *ab initio* capacity at the quantum mechanical level.

Following the original work by Cho *et al.*,[1] there have been several subsequent works of using wavelets on the pseudopotential calculations and introducing different wavelet basis functions.[7–10] However, a systematic test of the accuracy and efficiency of using wavelets for many-electron systems has not been performed yet. In this work, we apply the wavelet basis to the all-electron calculations and perform an extensive and systematic analysis to establish the efficiency and the accuracy of wavelets in the all-electron density-functional calculations.

Basic formalism for wavelet. We briefly discuss the mathematical background of the wavelet. We direct readers to other references for more complete discussions.[1,11] Given the $L^2(\mathbf{R}^3)$ space, the multiresolution analysis (MRA) is based on the hierarchical ladder structure of the *approximation* spaces:

$$\cdots V_{-2} \subset V_{-1} \subset V_0 \subset V_1 \subset V_2 \cdots = L^2.$$

There is a ''scaling function'' ϕ whose discrete translations span each approximation space; $V_j = \mathrm{span}\{\sqrt{2^j}\phi(2^j\mathbf{r}-\mathbf{n}); \mathbf{n}\in\mathbf{Z}^3\}$. One can define a *wavelet* space W_j as $V_{j+1}=V_j \oplus W_j$ so that W_j describes the details at resolution level $j+1$. W_j is expanded by a ''wavelet'' function ψ in the similar manner for the scaling function.

In principle, there are infinite number of different wavelets satisfying the above conditions. Until now, only a few wavelets are tested for the electronic structure calculation.[1,7–10] The orthogonality and the fast wavelet transform in the Daubechies wavelet facilitate the computation, but its singular shape prevents the significant reduction

in the number of bases compared to the PW, even with a soft pseudopotential.[7,8] On the other hand, the nonorthogonal Mexican hat wavelet adopted in this work is a second derivative of the Gaussian function and has a smooth shape suitable for expanding the Hamiltonian and wave functions.[12] Its scaling function can also be approximated as a Gaussian.[1,13] Another merit of the Mexican hat wavelet is that the Hamiltonian matrix can be constructed analytically except for the exchange-correlation term (see below). Since the Mexican hat wavelet is an overcomplete basis, there exist many different descriptions of a function in an exact sense. However, we pratically use only a portion of the wavelet space and the ''best'' description of the wave function is uniquely determined within the selected basis. Actually, we do not find any numerical instability caused by the overcompleteness in the following calculations.

The number of bases in MRA corresponding to a specific spatial region increases 8 times per one resolution increment and the selection of an optimal basis set at each resolution level is inevitable for the practical applications. In this work, we follow the original strategy of Cho *et al.*[1] and introduce the support spheres centered at each atomic position. Such an atom-based approach takes into account the fact that the electron wave functions possess high spatial frequencies mainly near the nucleus. Specifically, we keep a dyadic variation of the support radii $R_j = R_0 \cdot 2^{-j} (j = 0, 1, 2, \cdots, j_{max})$. This form provides a solid reference in the various examples studied here.

At the jth level, there are two extreme choices of the basis set V_j and $V_0 \oplus W_1 \oplus W_2 \oplus \cdots \oplus W_j$. Because the support radii are finite, they are not exactly equivalent. To gauge the effects of this difference, we have performed several test calculations, and the two choices show only slightly different convergence profiles as a function of R_0 and j_{max}.[14] Using only the scaling function simplifies many analytical integrations whereas the wavelet plus scaling function is more natural for the concept of systematic approximation. It is interesting to note that the Gaussian program in quantum chemistry can be viewed as a special case of using scaling functions without MRA.

Construction of Hamiltonian. The Hamiltonian with the local density approximation (LDA) (Ref. 15) is written in the atomic unit as follows:

$$H = -\frac{1}{2}\nabla^2 - \sum_{\text{nucleus},j} \frac{Z}{|\mathbf{r} - \mathbf{R}_j|} + V_{xc}[\mathbf{r}; n(\mathbf{r})] + \int \frac{n(\mathbf{r}')}{|\mathbf{r} - \mathbf{r}'|} d\mathbf{r}', \quad (1)$$

where $n(\mathbf{r})$ indicates the electron density. In order to minimize the numerical integrations involved in the exchange-correlation part, we fit V_{xc} with the wavelet basis and evaluate all the matrix elements analytically. This is one of the benefits of using the complete wavelet basis expanding $L^2(\mathbf{R}^3)$ space. The maximum resolution for V_{xc} can be reduced since V_{xc} varies more slowly than the wave functions. The overlap integral between a basis function and V_{xc} is evaluated through the conventional Gaussian quadratures adopting $30^3 - 60^3$ mesh points. Smaller quadrature points are sampled for the higher level wavelets with a narrow width. More sophisticated meshes designed for the electronic structure calculation can also be applied to save the computational
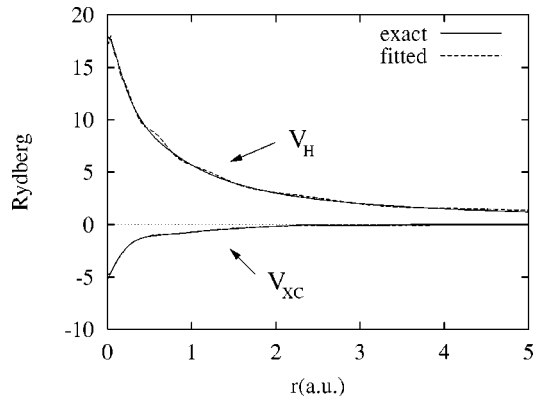

FIG. 1. Comparison between the fitted and the numerical shapes of the Hartree and the exchange-correlation potential for the carbon atom. Spherical symmetry is assumed.

time.[16] In Fig. 1, the numerical and the fitted V_{xc} for the carbon atom are compared, showing excellent agreement.

Keeping the analytic form of the density requires a double summation over the basis functions which is computationally very expensive for a large basis set. We avoid the double summation by projecting the charge density onto the basis set of the wave function under the fixed total charge. For a carbon atom, the squared difference between the exact and the projected densities is integrated to be 0.0004 in a.u. under a proper basis set (see below). This difference is negligibly small, and two densities cannot be visually discriminated.

It is also possible to fit the Hartree potential, the last term in the Hamiltonian (1). It reduces the computational load in generating the error function. It is found that the inclusion of one or two negative resolution levels (i.e., coarser resolution levels with larger support radii) improves the description of the long range tail in the Hartree potential (see Fig. 1).[17] It should be noted that these additional wavelets do not change the size of the Hamiltonian matrix. After the above preliminary steps, the evaluation of the matrix elements can be done very efficiently. We have used the conventional least-squares fits for each fitting procedure. In addition, the self-consistent electronic iterations are accelerated by the nonlinear Broyden mixing of input and output densities.[18]

Test on atoms and molecules. We take a simple cubic grid with the spacing of 2 a.u. for the coarsest level $(j=0)$. In order to determine the optimal R_0 and j_{max}, we perform the test calculations for each element with a simplified Hamiltonian neglecting electron-electron interaction. In Table I, we list R_0 and j_{max} for the minimal basis set reproducing the exact eigenvalues for the filled states within 0.1 eV. In addi-

TABLE I. Parameters for a minimal basis set necessary for the 0.1 eV accuracy in the eigenvalues of pseudoatoms without the electron-electron interaction.

Element	R_0(Å)	j_{max}	N_{basis}
H	3.0	2	55
C	4.8	7	407
O	4.9	8	673
Mg	5.0	10	881
Si	5.0	11	1057

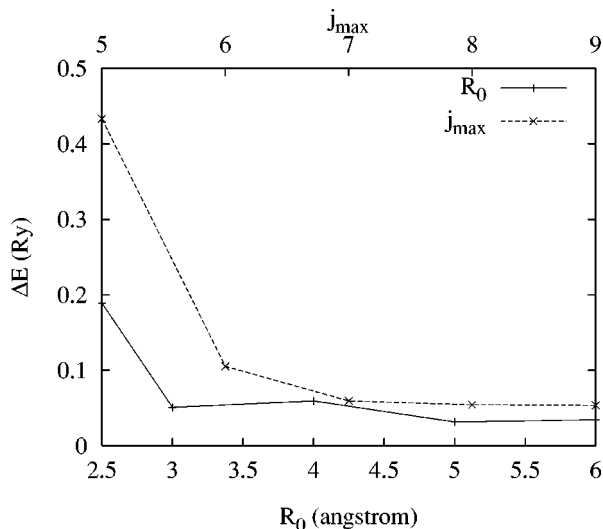FIG. 2. Errors in the total energy ($=E_{tot}^{wavelet}-E_{tot}^{1-d}$) of the C atom with respect to the maximum resolution level (j_{max}) as well as the support radius for the base level (R_0).

tion to the dyadic contraction, the support radii undergo some adjustments for the optimal choice of the basis set. It is meaningful to restate the resolution level in terms of the corresponding energy cutoff in a PW calculation. From the reconstruction of the PW with the Mexican hat wavelet,[13] the effective energy cutoff for the jth resolution level can be defined as $E_{cut}^{eff}\simeq(2/a_0)^2\times4^j$ Ry, where a_0 is the grid spacing in a.u. at $j=0$. At $j=7$ with $a_0=2$ a.u., the E_{cut}^{eff} is 16 000 Ry which corresponds to 20 million PW's in a $[7\text{ Å}]^3$ cubic box.

Based on the parameters in Table I, we perform the LDA calculations on the atoms and molecules. In Fig. 2, we show the convergence of the LDA total energy with respect to the resolution level and the support radius. The reference value is calculated with the one-dimensional atom code assuming the spherical symmetry. It is found that increasing the j_{max} changes mainly the core states whereas the overall improvements are achieved by expanding R_0. The conjugate-gradient method is used for determining the equilibrium geometry of molecules. Vibrational frequencies for H_2 and CO are obtained from the Murnaghan equation of state.[19] The calculated results are listed in Table II. They are in good agreement with experiments and other theoretical works. In the case of CO, we have also tested the effect of increasing the resolution level around the center of molecule for a more accurate description of the covalent bonding, but the results are almost unchanged. This indicates that the support radii determined in the atomic configuration are transferable to different environments. Figure 3 shows the Hellmann-Feynman forces on each atom in the H_2 molecule. The solid line is obtained by differentiating of the fitted Murnaghan's equation with respect to the interatomic distance. The overall coincidence in Fig. 3 implies the absence of the Pulay effect, consistent with the fact that the basis function in MRA is fixed as the atoms move. In Fig. 4, the σ-bonding states of the CO molecule are displayed. The almost cusplike peaks at the atomic sites are clearly visible. This figure demonstrates the ability of the Mexican hat wavelet in describing sharp structures.

TABLE II. Calculated physical quantities for various molecules. [d: equilibrium distance in Å, ω_0: harmonic frequency in cm^{-1}, E_c: cohesive energy in eV (zero point energy is not considered).]

		This work	Other work[a]	Exp.
	d(H-H)	1.434	1.446	1.401
H_2	ω_0	3951	4188	4400
	E_c	4.94	4.91	4.75
	d(C-O)	2.14	2.13	2.13
CO	ω_0	2172	2181	2170
	E_c	13.16	12.94	11.23
	d(H-O)	1.83	1.83	1.81
H_2O	$\angle$(H-O-H)	104.0°	104.9°	104.5°
	E_c	11.95	11.64	10.17

[a]Ref. 15.

Since the basis function is analytic, the implementation of the generalized gradient approximation (GGA) is easily done. We have used a recently proposed form of GGA (Ref. 20) to see the difference between the LDA and GGA. In Table III, the results for H_2 with the LDA and GGA are displayed. It is observed that the GGA in general improves the data toward the experimental values.

As a more stringent test, we have calculated the $1s$ core-ionization potentials for the CO molecule with the same basis as was used for the neutral case. The theoretical ionization potential is the difference between the GGA total energy of a molecule in the presence of a core hole and that of the neutral molecule. The spin-polarization effects are included through the local spin density functional. The calculated results are 540.6 and 295.0 eV for CO* and C*O, respectively. These are in excellent agreement with the experimental values 542.6 and 296.2 eV,[21] demonstrating that the effects of relaxations in the core and valence orbitals due to the hole creation are properly described by the given basis set.

The main computational bottleneck in the current implementation of the wavelet lies in the evaluation of the matrix
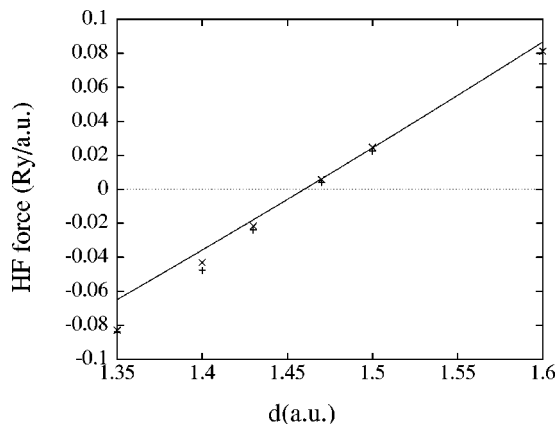

FIG. 3. Hellmann-Feynman forces on the atoms of the H_2 molecule with respect to the interatomic distance. The solid line is a derivative of the fitted Murnaghan equation of state, and $\times$ and $+$ are for the left and right H atoms, respectively. The sign of the force on the right H atom has been reversed for convenience in presentation.
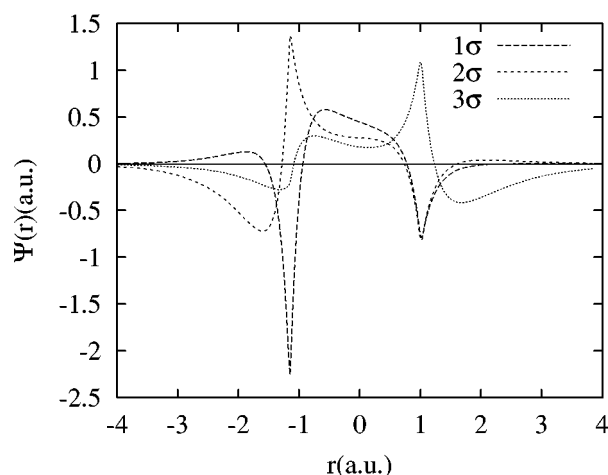
FIG. 4. Wave functions for the σ-bonding states in the CO molecule with the interatomic distance 2.15 a.u. The orbitals are numbered according to the magnitude of eigenvalues. The origin of the abscissa coincides with the bond center.

TABLE III. Calculated quantities of H_2 when GGA is used and the GGA-induced changes from the LDA results in Table II.

	GGA	Changes (this work)	Changes (other work[a])	Exp.
d(H-H) (Å)	1.402	-0.032	-0.029	1.401
ω_0 (cm^{-1})	4122	171	135	4400
E_c (eV)	4.53	-0.41	-0.37	4.75

[a]Ref. 15.

calculations with the LDA and GGA. By systematically testing the resolution levels and the support radii, uniform convergence in the total energy is achieved to the desired accuracy despite the wide range of the energy spectrum of the filled electronic states. The control of the resolution levels according to the individual atomic Coulomb potential makes it possible to select the basis components for general applications. It is found that the test with the hydrogenlike atom model provides a good reference for the basis parameters. The projections of the potentials and the density onto the wavelet bases greatly enhance the computational efficiencies. We are currently investigating the applications of the Mexican hat to the pseudopotential calculation and the $O(N)$ methods.

elements. This is mainly due to the nonorthogonality of the Mexican hat wavelet. For a large scale simulation, one may exploit a tight frame of the wavelet for neglecting overlap integrals between the wavelets far apart. The $O(N)$ method[4] is also a promising application field of the wavelet. As shown above, higher resolutions are necessary mainly for the core states which are usually not involved in the chemical bonding. We expect that a further reduction in the basis size can be achieved by freezing the core electrons and lowering the j_{max} for the valence states.

Summary. We have developed and applied the Mexican hat wavelet electronic structure program to the all-electron

[1] K. Cho, T. A. Arias, J. D. Joannopoulos, and P. K. Lam, Phys. Rev. Lett. **71**, 1808 (1993); K. Cho, Ph.D. thesis, Massachusetts Institute of Technology, 1994.

[2] F. Gygi, Europhys. Lett. **19**, 167 (1992); A. Devenyi, K. Cho, T. A. Arias, and J. D. Joannopoulos, Phys. Rev. B **49**, 13 373 (1994).

[3] N. A. Modine, G. Zumbach, and E. Kaxiras, Phys. Rev. B **55**, 10 289 (1997); E. L. Briggs, D. J. Sullivan, and J. Bernholc, *ibid.* **52**, R5471 (1995).

[4] W. Yang, Phys. Rev. Lett. **66**, 1438 (1991).

[5] F. F. Abraham, J. Q. Broughton, N. Bernstein, and E. Kaxiras, Nature (London) (to be published).

[6] The periodic boundary condition does not allow a general nonperiodic deformation of the supercell so that the PW program cannot be embedded within atomistic simulations.

[7] S. Wei and M. Y. Chou, Phys. Rev. Lett. **76**, 2650 (1997).

[8] C. J. Tymczak and X. Wang, Phys. Rev. Lett. **78**, 3654 (1997).

[9] M. E. Brewster, G. I. Fann, and Z. Yang, J. Math. Chem. **22**, 117 (1997).

[10] T. A. Arias, Rev. Mod. Phys. **71**, 267 (1999).

[11] I. Daubechies, *Ten Lectures on Wavelets* (Society for Industrial and Applied Mathematics, Philadelphia, 1992); C. K. Chui, *An Introduction to Wavelets* (Academic Press, San Diego, 1992).

[12] Mathematically, MRA is constructed on the orthonormal wavelet. However, the main idea of MRA relevant to the physical problems is the decomposition of a function with a localized basis set that is assorted according to the spatial frequency, and this is maintained in Mexican hat as shown in the text.

[13] T.A. Arias, K.J. Cho, P.K. Lam, and M.P. Teter, in *Toward Teraflop Computing and New Grand Challenge Applications*, edited by P. K. Kalia and P. Vashishta (Nova Scientific Publications, Commack, 1995), p. 23.

[14] For example, in the case of H^{2+} considered in Ref. 1, the difference in energy is less than 0.01 eV.

[15] P. Hohenberg and W. Kohn, Phys. Rev. **136**, B864 (1964); W. Kohn and L. J. Sham, *ibid.* **140**, A1133 (1965).

[16] D. C. Patton, D. V. Porezag, and M. R. Pederson, Phys. Rev. B **55**, 7454 (1997); M. R. Pederson and K. A. Jackson, *ibid.* **41**, 7453 (1990).

[17] In a rigorous sense, the Hartree field does not belong to the L^2 space. However, in practice, it can be expanded in wavelets, and the wavelet description fails only at a large distance compared to the outermost support boundary. Introduction of coarser resolutions reduces already small errors in this approximate expansion.

[18] C. G. Broyden, Math. Comput. **19**, 577 (1965).

[19] F. D. Murnaghan, Proc. Natl. Acad. Sci. USA **3**, 244 (1944).

[20] J. P. Perdew, K. Burke, and M. Ernzerhof, Phys. Rev. Lett. **77**, 3865 (1996).

[21] L. Triguero, L. G. M. Pettersson, and H. Agren, Phys. Rev. B **58**, 8097 (1998), and references therein.